Precise Attitude Control of All-Electric GEO Spacecraft using Xenon Microthrusters

IEPC-2013-070

Presented at the 33rd International Electric Propulsion Conference,
The George Washington University, Washington, D.C., USA
October 6–10, 2013

Mirko Leomanni*, Andrea Garulli† and Antonio Giannitrapani‡
Università di Siena, Siena, 53100, Italy

Fabrizio Scortecci§
Aerospazio Tecnologie s.r.l., Rapolano Terme, Siena, 53040, Italy

This paper addresses the problem of precise pointing for a small all-electric GEO platform. The attitude control system is based on cold gas and electrothermal Xenon microthrusters, sharing a common propellant bus with the primary electric propulsion system. The considered technology requires that restrictions on the duration and number of thruster firings are taken explicitly into account in the design of the control law. To this aim, a receding horizon model predictive control scheme is proposed, whose cost functional allows one to suitably trade-off fuel consumption and number of firing cycles. The viability of the approach is demonstrated on a GEO mission with high pointing and pointing rate accuracy requirements.

I. Introduction

Spacecraft systems using geostationary orbit (GEO) have a high commercial and strategic value, thanks to the ability to provide continuous coverage over a wide geographical area. The vast majority of communication satellites and an increasing number of Earth observation missions are in fact designed to operate in GEO, see e.g. [1, 2]. The recent growth of satellite communication services has imposed severe restrictions on the size and the number of free GEO locations. At the same time, many scientific organizations have suffered from budget limitations. As a consequence, commercial platforms with shared communications and observation payloads have received considerable interest, providing a consistent, dependable and affordable access to space [3, 4]. In order to meet the mission requirements imposed by multiple payloads, satellite operators are demanded to constantly upgrade the performance of their systems.

All-electric spacecraft seems to be one of the most promising concepts to enable high performance GEO missions at a substantially decreased cost compared to conventional platforms. This is achieved through the considerable reduction of spacecraft mass and size allowed by the use of high efficiency electric propulsion (EP) systems for orbit raising and station-keeping (SK) operations [5, 6]. Several solutions are still under investigation to provide precise attitude control of all-electric spacecraft, as required for operation of advanced communications and Earth observation payloads. Momentum exchange devices, such as ball-bearing reaction wheels and control moment gyros, are by far the most commonly used actuators. Their main advantage is that a minimum amount of fuel is needed to counteract attitude perturbations, in particular when momentum dumping is conveniently performed during SK maneuvers, using EP thrusters [7]. Nevertheless, microvibrations associated with wheel unbalance, zero-rate crossing and friction instabilities represent serious drawbacks of these systems, especially for applications that require high pointing accuracy. In addition,

*Ph.D, Dipartimento di Ingegneria dell'Informazione e Scienze matematiche, leomanni@dii.unisi.it.
†Professor, Dipartimento di Ingegneria dell'Informazione e Scienze matematiche, garulli@dii.unisi.it.
‡Assistant Professor, Dipartimento di Ingegneria dell'Informazione e Scienze matematiche, giannitrapani@dii.unisi.it.
§Chairman, Aerospazio Tecnologie s.r.l., fscortecci@aerospazio.com.

momentum exchange devices tend to be costly, massive, and require a large amount of power. As an attempt to solve some of these issues, a wheel-less EP-based attitude control system (ACS) has been proposed in [8], although it has been found not to be viable for the specific case of the scientific mission GEO-Oculus [9]. A solar pressure attitude control concept has been successfully experimented on a class of GEO satellites, but there exist several practical implementation problems to be resolved prior to a large-scale application of this advanced technique [10].

Reaction control systems based on Xenon thrusters, sharing a common propellant bus with the primary EP system, represent another viable solution, that could be beneficial to reduce development complexity and costs of all-electric spacecraft. Cold gas and electrothermal microthrusters, with thrust levels scaled down to the millinewton range, are particularly well suited for precise attitude control, providing very small impulse bits and a minimal excitation of the spacecraft flexible modes. While the poor fuel efficiency of cold gas systems restricts their use to operational environment where the delta-v budget is considerably low, the foreseen availability of very high temperature resistojet and hollow cathode technologies, providing a substantial increase of the thruster specific impulse, raises the possibility of replacing existing momentum exchange devices with simple, reliable and relatively inexpensive Xenon microtrusters [11, 12]. However, these thrusters are typically operated in on/off mode, and restrictions on the duration and number of thruster firings have to be accounted for in the design of the ACS.

In this paper, the application of a microthruster reaction system is proposed for three-axis precision pointing of a small all-electric spacecraft orbiting in GEO. To this aim, a novel approach to ACS design is presented, whose objective is to keep the spacecraft attitude close to the nominal Earth pointing attitude within tight bounds, providing an efficient compensation of the disturbance torques, while optimizing the performance of the propulsion system in terms of fuel consumption and number of firing cycles. The computation of the control law requires the on-line solution of a constrained optimization problem, according to a receding horizon model predictive control (MPC) strategy. Simulations of a realistic spacecraft model are reported to demonstrate the feasibility of the proposed solution.

The paper is organized as follows. Section II presents the reference mission. Section III describes the spacecraft layout and the main features of the proposed ACS. In Section IV, the spacecraft dynamic model is introduced, along with a detailed analysis of the disturbance torques acting on the spacecraft. In Section V, the attitude determination and control system is presented. The performance of the proposed microthruster reaction system is evaluated through simulation tests in Section VI. In Section VII, some conclusions are drawn and future directions of research are outlined.

II. Reference mission

The objective of the reference mission is to provide high accuracy attitude control of a small all-electric GEO platform, for a mission duration of 15 years, after the orbit raising phase. Table 1 shows the nominal values of the orbital elements for an example GEO slot. The nominal attitude is Earth pointing, such that the spacecraft body frame is aligned with a local-vertical/local-horizontal (LVLH) frame centered at the spacecraft center of mass. The roll, pitch and yaw axes of the body frame are the principal axes of inertia of the spacecraft. The Z axis of the LVLH frame is aligned with the nadir vector, the Y axis is normal to the orbital plane and points towards south, and the X axis completes an orthogonal right handed coordinate system.

Table 1. GEO reference slot

Semi-major axis	a	$= 42165$ (km)
Inclination	i	$\in [\,0\,,\ 0.05\,]$ (deg)
Longitude	λ	$\in [\,75.05\,,\ 75.15\,]$ (deg)
Eccentricity	e	$\simeq 0$

The most significant disturbance effect on the spacecraft position is the luni-solar perturbation, which causes a precessional motion of the orbital plane characterized by an initial secular drift of the inclination, while minor perturbations due to both Earth's gravity and solar radiation pressure affect the satellite longitude and the orbit eccentricity. As a consequence, maintaining the spacecraft inside the assigned slot requires

periodic SK maneuvers, to be performed using EP thrusters. The principal attitude disturbances are a persistent SK torque, which is generated during SK maneuvers due to unavoidable misalignment of the EP thrust vector with respect to the spacecraft center of mass, and the environmental torques, arising from the interaction of environmental perturbations with the mass distribution and the geometric properties of the spacecraft. To counteract the attitude drift due to disturbance torques, real-time attitude control is needed.

The attitude control accuracy requirements for the considered GEO platform are dictated by the type of payload carried onboard. A shared payload configuration is considered, including Ka/Ku-band communication instruments and Earth imaging devices. While a pointing accuracy below a given value is the driving requirement for telecommunications, an additional requirement on the pointing rate accuracy has to be met for Earth observation, which is typically performed during some fractions of the orbit. Since the pointing stability of the spacecraft is affected by SK maneuvers, Earth imaging is not performed during such operations. It is hence assumed that communications instruments are always active, and that the spacecraft is ready to perform Earth observation during most of the orbital period, except from the time needed for SK operations, during which pointing rate accuracy requirements are relaxed. The configuration in which SK maneuvers are not performed is referred as free orbit drift. Moreover, control accuracy requirements for the yaw axis are less stringent than those for the roll and pitch axes, because the yaw pointing error does not directly affect the quality of communications and observations. The attitude control specifications are summarized in Table 2, according to the typical requirements of a multi-mission platform, see e.g. [13].

Table 2. Attitude control requirements

ACS requirements	Free orbit drift		Station-Keeping	
	Roll, Pitch	Yaw	Roll, Pitch	Yaw
Pointing accuracy	0.5 (mrad)	1 (mrad)	0.5 (mrad)	1 (mrad)
Pointing rate accuracy	1.5 (μrad/s)	3 (μrad/s)	10 (μrad/s)	20 (μrad/s)

III. Spacecraft layout and power system

The spacecraft external layout is representative of a typical two tons small geostationary platform, see e.g. [14]. The size of the main body is $2\,\mathrm{m} \times 2\,\mathrm{m} \times 2.5\,\mathrm{m}$ and two solar panels of dimensions $5\,\mathrm{m} \times 2\,\mathrm{m}$ are attached to the north and south faces of the bus, providing 4.5 kW of average power. The considered propulsion system is illustrated in Figure 1. Four SPT-100 Hall effect thruster (HET) modules (EP1, EP2, EP3, EP4) symmetrically oriented around the nadir vector, with an angle of 45° between the north/south axis and the thrust direction, are used for GEO orbital maneuvers. Nominally, the EP thrust vectors are aligned with the center of mass of the spacecraft. Eight on/off Xenon microthruster modules that can be operated either as cold gas thrusters (CGT) or high temperature electrothermal thrusters (HTET) are used for real-time attitude control. Operation in HTET mode provides an increased specific impulse (I_{sp}), which is expected in the 100 s region for both high temperature resistojets and hollow cathode thrusters using Xenon [15]. Four thrusters (AT1, AT2, AT3, AT4) are mounted on the anti-nadir face, with an angle of 48.5° between the diagonal of the face and the thrust direction, to maximize the lever arm and hence the torque about both the roll and pitch axes. The remaining four thruster (AT5a, AT5b, AT6a, AT6b) are symmetrically oriented around the nadir vector, with an angle of 135° between the north/south axis and the thrust direction, and fired in pairs to provide pure torques around the yaw axis. Such configuration is fully compatible with thruster plume direction, torque level and power requirements of the considered mission. To avoid control torques summing up to zero, the simultaneous use of thrusters AT1-AT4, AT2-AT3 and AT5-AT6 is prevented. The basic specifications of the propulsion system are summarized in Table 3.

The layout of the attitude control thrusters has been designed to provide an efficient rejection of the SK disturbance torque generated by uncertainty on the center of mass and EP thruster misalignment. For any possible combination of the actual center of mass position and EP thrust directions, the pitch and roll components of such disturbance are coupled and have approximately the same magnitude, while the yaw component, with a larger worst-case magnitude, is almost decoupled. The force generated by the attitude control thrusters mounted on the anti-nadir face is found to have negligible impact on the spacecraft orbit,

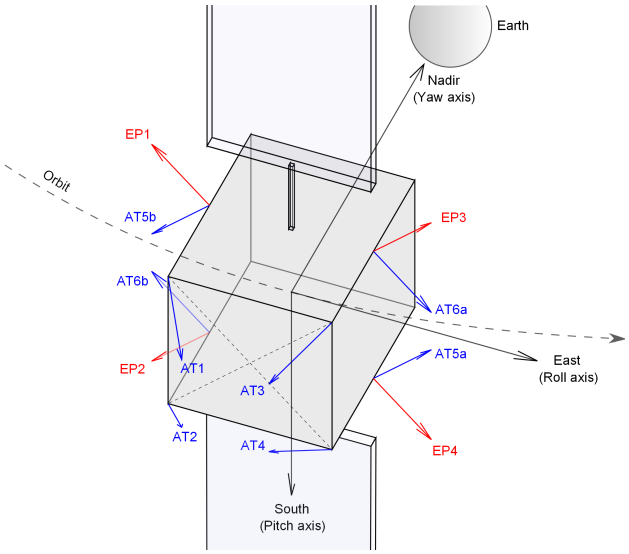

Figure 1. Thrusters location

so that an eventual long-term contribution is easily compensated by sporadic EP maneuvers.

Table 3. Propulsion system specifications

Type	Thrust	I_{sp}	Min. firing Time	Power	Mass
HET	75 (mN)	1500 (s)	>10 (min)	1350 (W)	3.5 (kg)
CGT/HTET	0.5/1.5 (mN)	30/90 (s)	>0.05 (s)	<60 (W)	<0.3 (kg)

IV. Attitude dynamic model

The coordinate systems used for the definition of the attitude dynamic model are the spacecraft body-fixed frame and the Earth centered inertial (ECI) frame. Rotations between these frames are expressed by quaternions $\mathbf{q}$. The scalar portion of the quaternion is the first element and the quaternion multiplication is denoted with the symbol $\circ$. Let $\mathbf{q}_{IB}$ be the quaternion representing the orientation of the spacecraft body frame with respect to the ECI frame, and $\boldsymbol{\omega}$ be the angular rate of the body frame with respect to ECI frame, expressed in the body frame. The model describing the attitude dynamics can be written as

$$\dot{\mathbf{q}}_{IB} = \frac{1}{2}\begin{bmatrix} 0 \\ \boldsymbol{\omega} \end{bmatrix} \circ \mathbf{q}_{IB}\,, \tag{1}$$

$$\dot{\boldsymbol{\omega}} = \mathbf{I}_{\mathrm{M}}^{-1}\Big(\boldsymbol{\tau}_d + \boldsymbol{\tau}_u - \boldsymbol{\omega} \times \mathbf{I}_{\mathrm{M}}\,\boldsymbol{\omega} - \dot{\mathbf{I}}_{\mathrm{M}}\,\boldsymbol{\omega}\Big)\,, \tag{2}$$

where $\mathbf{I}_{\mathrm{M}}$ is the spacecraft inertia matrix, $\boldsymbol{\tau}_d$ is the disturbance torque and $\boldsymbol{\tau}_u$ is the control torque (both expressed in the body frame). The most significant disturbance torques for the reference mission are the environmental disturbance torque $\boldsymbol{\tau}_e$, caused by the gravity gradient and the solar radiation pressure, and the disturbance torque $\boldsymbol{\tau}_{sk}$ acting on the satellite during SK operations. Since thrusters AT5a and AT5b, as well as thrusters AT6a and AT6b, are fired simultaneously, denoting by $\boldsymbol{\tau}_5$ and $\boldsymbol{\tau}_6$ the corresponding resulting torques, the mapping between the control torque $\boldsymbol{\tau}_u$ and the on/off activation command $\mathbf{u}$ is given by:

$$\boldsymbol{\tau}_u = \mathbf{T}\mathbf{u} = \begin{bmatrix} \boldsymbol{\tau}_1 & \boldsymbol{\tau}_2 & \boldsymbol{\tau}_3 & \boldsymbol{\tau}_4 & \boldsymbol{\tau}_5 & \boldsymbol{\tau}_6 \end{bmatrix} \mathbf{u}\,, \tag{3}$$

where $\mathbf{u} = [\, u_1\,,\ \ldots\,,\ u_6\,]^T$, with $u_i \in \{0,\, 1\}$. Given the thruster alignments, the matrix $\mathbf{T}$ has the following structure

$$\mathbf{T} = \bar{f} \begin{bmatrix} -d_{xy} & d_{xy} & -d_{xy} & d_{xy} & 0 & 0 \\ d_{xy} & d_{xy} & -d_{xy} & -d_{xy} & 0 & 0 \\ 0 & 0 & 0 & 0 & d_z & -d_z \end{bmatrix}, \tag{4}$$

where $\bar{f}$ is the nominal thrust magnitude and d_{xy}, d_z are constant lever arms. Due to the thruster layout design, coupled control torques of equal magnitude are produced around the roll and pitch axes, while the control torque around the yaw axis is decoupled. The propellant mass rate, resulting from thruster operation, is

$$\dot{m} = -\frac{\bar{f}\,\|\,\mathbf{\Lambda}\,\mathbf{u}\,\|_1}{g\,I_{sp}}\,, \tag{5}$$

where g is the gravity acceleration, the matrix $\mathbf{\Lambda} = \mathrm{diag}([1,\, 1,\, 1,\, 1,\, 2,\, 2])$ accounts for the specific thruster configuration and

$$\|\,\mathbf{x}\,\|_1 = \sum_{i=1}^{n} |\,x_i\,| \tag{6}$$

is the 1-norm of a vector $\mathbf{x} \in \mathbb{R}^n$.

A detailed analysis of the disturbance torques acting on the satellite is performed. The gravity gradient torque is usually negligible at GEO altitude, since it decreases with the inverse cubic power of the distance from the Earth [16]. The solar radiation pressure torque varies depending on the orientation of the solar panels. Since the solar panels rotate at a rate of one rotation per day to track the Sun, the resulting disturbance is characterized by daily quasi-periodic oscillations with an amplitude that depends on the offset between the center of mass of the spacecraft and the center of solar pressure. Moreover, this disturbance is set to zero during eclipses.

The disturbance torque, arising from station keeping operations, depends on both the offset of the center of mass with respect to the nominal position and the misalignment of the EP thrust vector from the nominal direction. The uncertain position of the center of mass and center of pressure as well as the thrust vector misalignment are accurately modeled for the attitude dynamics simulation, and assumed to be constant during each simulation. By simulating a weekly station-keeping cycle, with one day devoted to orbit determination followed by six days of pre-planned maneuvers (see e.g. [7]), it turns out that the maximum magnitude of the SK disturbance torque $\boldsymbol{\tau}_{sk}$ is much greater than that of the environmental torques $\boldsymbol{\tau}_e$. Only north/south maneuvers, which represents about 95% of the total SK delta-v budget, are considered in this study. The geometry of the maneuver is depicted in Fig. 2, where the EP thrusters are fired near the orbit nodes. During most of the orbital period, the spacecraft is allowed to drift with respect to the nominal orbit and experiences small environmental torques only, while a significant persistent torque is generated during orbit correction maneuvers. This is clearly visible in Fig. 3, which shows the daily behaviour of the disturbance torques, expressed in the spacecraft body frame, for a typical simulation (notice the different magnitudes of the torques).

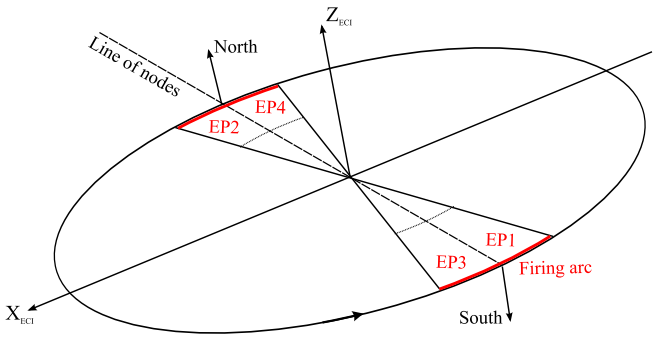

Figure 2. North/south station-keeping maneuver

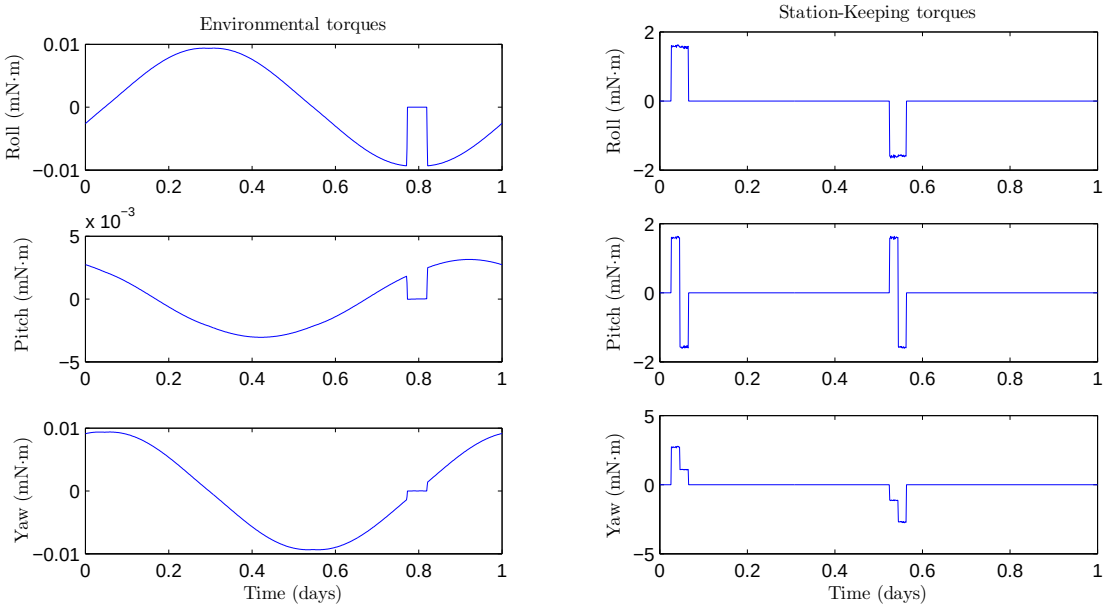

Figure 3. Disturbance torques: $\boldsymbol{\tau}_e$(left), $\boldsymbol{\tau}_{sk}$(right)

V. Attitude control

The purpose of the ACS is to track the LVLH reference trajectory, which is periodically uploaded from ground, within the prescribed accuracy. The most significant limitations of the microthruster reaction system are the low fuel efficiency and the maximum number of cycles which can be delivered by the switching valves during thruster lifetime. Since thrusters are designed to be possibly operated in electrothermal mode, by ohmic heating of a resistance element, the following operation regime is considered to retain an acceptable number of thermal cycles:

- CGT mode operation of AT thrusters for attitude control during free orbit drift, when a low delta-v is required to counteract the environmental torques.
- HTET mode operation of AT thrusters for attitude control during SK maneuvers, providing increased thrust and I_{sp} for efficient compensation of additional EP-induced torques.

Based on the linear discrete-time approximation of eqs. (1) and (2) around the reference trajectory (see, e.g., [17]), which is defined by the LVLH frame orientation $\bar{\mathbf{q}}_{IL}$ and its angular rate $\bar{\boldsymbol{\omega}}_L$, an MPC strategy [18] is derived for precise attitude control. The state of the linearized model includes the roll, pitch and yaw error vector $\delta\boldsymbol{\theta}$ and its derivative $\delta\boldsymbol{\omega}$:

$$\mathbf{x} = \left[\, \delta\boldsymbol{\theta}^T \,,\;\; \delta\boldsymbol{\omega}^T \,\right]^T. \tag{7}$$

The computation of the control law, which explicitly incorporates pointing and pointing rate accuracy requirements as well as performance indexes representing the fuel consumption and the number of thruster firings, requires the solution of the following constrained optimization problem:

$$\begin{aligned} \min_{\mathbf{U}_{t,N}} \quad & (1-\alpha)\, J_1(\mathbf{U}_{t,N}) + \alpha\, J_2(\mathbf{U}_{t,N}) \\ \text{s.t.} \quad & -\mathbf{x}_M \le \mathbf{x}\,(t+k+1\,|\,\mathbf{x}(t), \mathbf{U}_{t,k}\,, \boldsymbol{\tau}_d(t)) \le \mathbf{x}_M \quad \forall\, k = 0, \ldots, N \\ & u_i(t+k) \in \{0,\, 1\} \quad \forall\, i, \forall\, k = 0, \ldots, N\,, \end{aligned} \tag{8}$$

where the input sequence $\mathbf{U}_{t,N} = \{\mathbf{u}(t), \ldots, \mathbf{u}(t+N)\}$, which is mapped into corresponding control torques according to (3), is computed on a predefined control horizon N. The evolution of the state within the control horizon is defined by the linearized discrete-time attitude model as a function of the initial conditions and the control sequence, and denoted by $\mathbf{x}\,(t+k+1\,|\,\mathbf{x}(t), \mathbf{U}_{t,k}\,, \boldsymbol{\tau}_d(t))$. The vector $\mathbf{x}_M$ contains upper bounds

on the tracking error, accounting for the control accuracy specifications reported in Table 2. The parameter $\alpha \in [0, 1]$ is a relative weight of the fuel consumption J_1 and the number of thruster firings J_2 in the cost function. According to (5), the amount of expended fuel from time t to time $t + N$ is given by:

$$J_1(\mathbf{U}_{t,N}) = \sum_{k=0}^{N} \| \mathbf{\Lambda}\, \mathbf{u}(t+k) \|_1 . \tag{9}$$

Moreover, being $u_i \in \{0, 1\}$, the number of thruster switchings, which accounts for thruster valve wear, can be expressed as:

$$J_2(\mathbf{U}_{t,N}) = \sum_{k=0}^{N} \| \mathbf{\Lambda}[\mathbf{u}(t+k) - \mathbf{u}(t+k-1)] \|_1 . \tag{10}$$

Problem (8) is solved at each time t and the first element $\mathbf{u}(t)$ of the control sequence $\mathbf{U}_{t,N}$ is applied to the system, according to a receding horizon strategy. In order to solve problem (8) in real time, an estimate of the initial state $\mathbf{x}(t)$ and of the disturbance torque $\boldsymbol{\tau}_d(t)$ must be available. Since the disturbance torque depends on thruster misalignment and center of mass position, one can assume that it is constant over the considered control horizon and treat it as an uncertain parameter to be estimated. An extended Kalman filter (EKF) is used to estimate both the attitude and the disturbance torque, by using combined gyro and star-tracker measurements [19, 20]. The resulting closed-loop system is depicted in Figure 4, where $\hat{\mathbf{q}}_{IB}$, $\hat{\boldsymbol{\omega}}$ and $\hat{\boldsymbol{\tau}}_d$ denote the estimates of the spacecraft attitude, rotation rate and disturbance torque, respectively. Note that the estimated state $\hat{\mathbf{x}}(t)$ includes the three-dimensional rotation vector $\delta\hat{\boldsymbol{\theta}}(t)$ and the estimated angular rate of the spacecraft with respect to the LVLH rate, expressed in the body frame, $\delta\hat{\boldsymbol{\omega}}(t)$.

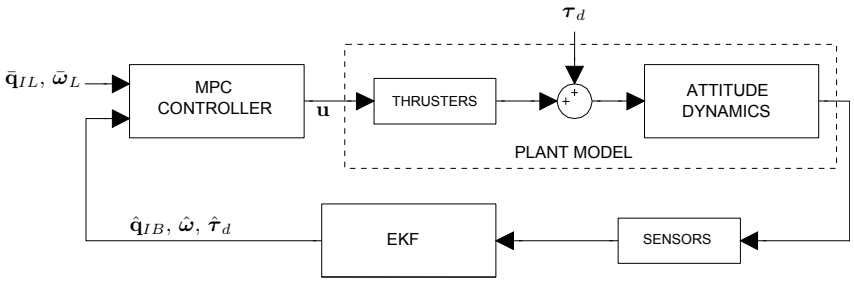

Figure 4. Closed-loop system

An advantageous feature of the MPC approach is that, once $\mathbf{x}_M$ and N are set, the value of the parameter α can be triggered to trade-off between the number of thruster firing cycles and the fuel consumption required for disturbance rejection. To find a suitable value of α, the ACS has been simulated with values of α ranging from zero to one. Since different control modes are defined according to mission requirements, free orbit periods lasting one day and SK maneuvers of 55 minutes duration have been simulated separately. A worst-case scenario has been considered, by assuming the maximum disturbance torque compatible with the uncertainty on the center of mass, center of solar pressure and thruster misalignment, as illustrated in Fig. 3. The results are depicted in Figure 5, where the fuel consumption and the number of thruster firings are reported for SK and free orbit drift periods. As expected, the parameter α allows one to trade-off two conflicting objectives. It can be noticed that for both SK and free orbit drift the fuel consumption is approximately constant as long as α is smaller than 0.8, while it rapidly grows as α approaches 1. Conversely, an acceptable number of firings is achieved only if α is larger than 0.7. From these observations, $\alpha = 0.75$ has been selected. Figure 5 also confirms that the major contribution to the attitude control delta-v budget is due to SK operations. Even if the microthrusters efficiency is increased by HTET mode operation, the fuel required for EP disturbance rejection of a single SK maneuver is still considerably higher than the fuel needed to compensate for one day of environmental torques using CGT mode.

VI. Simulation results

In order to evaluate the performance of the ACS and demonstrate the feasibility of the proposed solution, the reference GEO mission is numerically simulated for one week, according to the periodicity of the SK

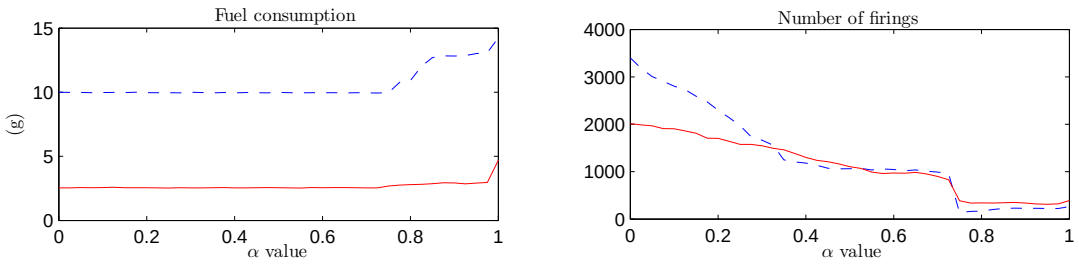

Figure 5. Tuning of parameter α for SK (dashed line) and free orbit drift (solid line)

cycle. To this purpose, a high-fidelity simulator has been developed, combining a realistic model of the spacecraft dynamics with a navigation system relying upon an EKF for state estimation. Uncertainty sources and disturbance effects, affecting the real spacecraft dynamics, are included in the simulation model. Both the spacecraft mass and inertia matrix are time-varying due to propellant expulsion and moving parts. The actual center of mass and the thruster alignment are allowed to differ from the nominal values. Disturbance accelerations due to solar radiation pressure, aspherical and third body gravity are taken into account. Disturbance torques resulting from gravity gradient, solar radiation pressure (taking into account the rotation of the solar panels) and EP thrusters misalignment are also considered. A multiplicative extended Kalman filter takes care of estimating the spacecraft attitude and angular velocity from star-tracker and gyro measurements. As an additional output, the EKF yields an estimate of the disturbance torque, which is used by the MPC controller. Table 4 summarize the fundamental features of the simulation, assuming a worst-case scenario.

Table 4. Simulation parameters

Parameter	Value
Center of mass offset	1.5 cm per axis
Center of solar pressure offset	5 cm along the pitch axis
EP thrust vector misalignment	0.6 deg half-cone
AT thrust vector misalignment	0.1 deg half-cone
EP and AT thrust noise	1 % of the nominal thrust
Gyro measurement noise	1 μrad/$\sqrt{\text{s}}$ (3σ)
Star-tracker measurement noise	0.1 mrad (3σ)
ACS rate	2 Hz

The effect of the weekly station-keeping cycle on the orbit inclination is depicted in Fig. 6, together with the Xenon mass expelled by the HET modules during prescribed north/south maneuvers. The orbit control system succeeds in keeping the spacecraft inside the assigned GEO slot, which is delimited by the dash-dotted line, and the orbit inclination is driven approximately back to the initial value. After the first day of free orbit drift, two orbit correction maneuvers per day are performed, requiring about 0.2 kg of propellant. Based on this data, 15 years of north/south SK operations would require approximately 159 kg of Xenon, which is in line with the results obtained for the Small-GEO platform using SPT-100 thrusters [1].

The ACS must guarantee tracking of the reference attitude and angular rate, while accounting for mission performance indexes such as fuel consumption and actuator wear. The attitude tracking error is reported in Fig. 7, in terms of the angular separation between the spacecraft orientation and the LVLH frame orientation with respect to the roll, pitch and yaw axes of the spacecraft body frame. The tracking error remains always well enclosed within the bounds (dash-dotted lines) specified by the pointing accuracy requirements, and shows an oscillating trend that corresponds to the disturbance torque profile most of the time, except from periodic spikes due to SK maneuvers and thruster operation within eclipses. Such kind of behaviour is typical for pulse-modulated thruster control systems with deadband [21]. The pointing rate error, defined as the angular rate of the spacecraft with respect to the LVLH rate expressed in the body frame, is depicted in

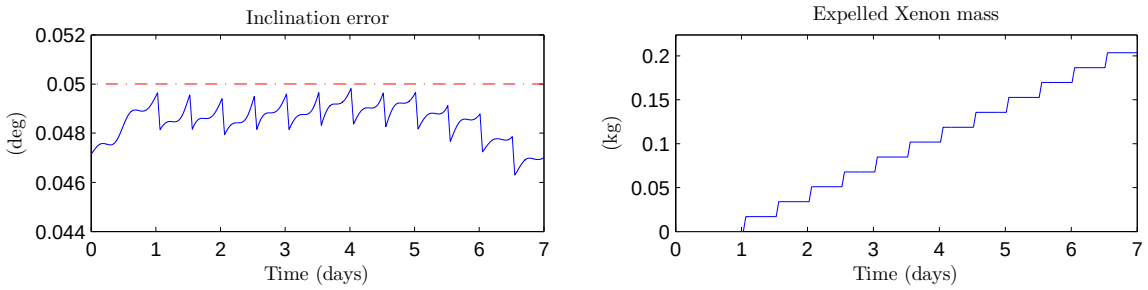

Figure 6. Weekly station-keeping cycle

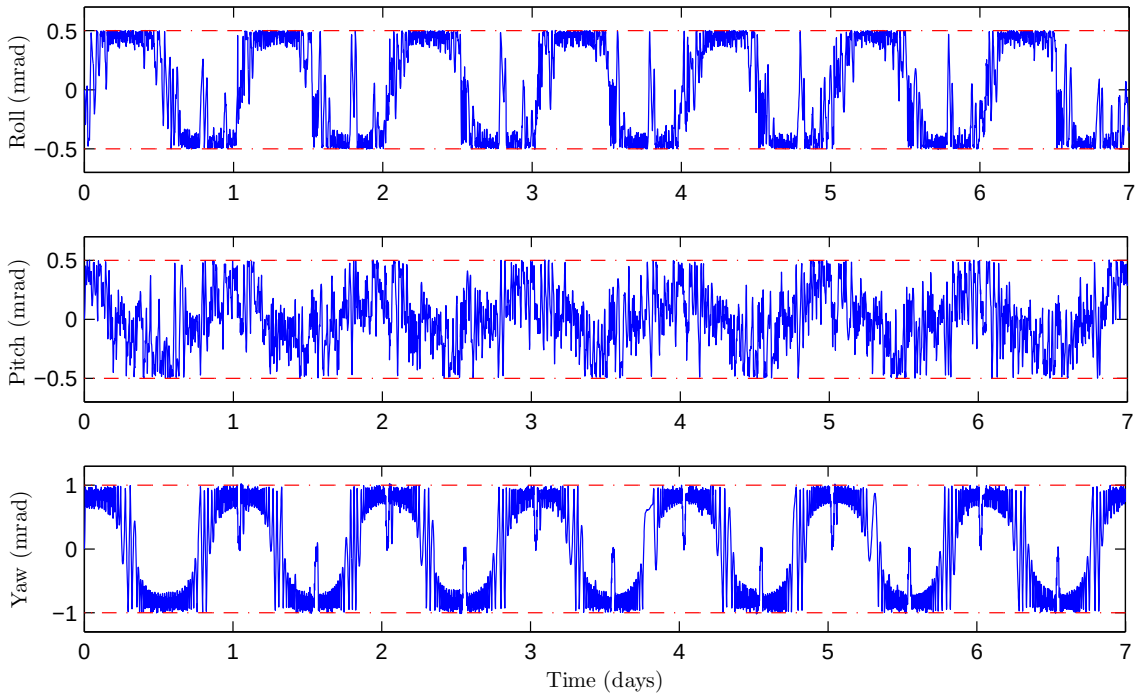

Figure 7. Pointing error

Fig. 8. Similarly to what observed for the attitude error, the angular rate error does not exceed the pointing rate accuracy bounds, which are relaxed during SK maneuvers to allow for a better management of the thruster firing cycles.

The performance of the microthruster reaction system, in terms of fuel consumption and number of firings cyles per thruster, is reported in Fig. 9. The microthrusters are operated in CGT mode during free orbit drift and in HTET mode during SK maneuvers. The stair-step profile of the expelled fuel clearly indicates that the major contribution to the propellant budget is due to SK maneuvers, as expected. The overall Xenon mass required for precise attitude control is approximately 0.135 kg: 0.019 kg to counteract environmental disturbances and 0.116 kg to compensate for EP torques. The amount of firing cycles is fairly distributed among free orbit drift and SK maneuvers, and grows regularly for each thruster. At the end of the simulation, about 800 on/off cycles are accumulated by thrusters AT1 and AT4, while a number of cycles between 600 and 650 is observed for the remaining thrusters. The overall firing time per thruster varies between 2.5 hr and 2.9 hr, about 85% of which being spent for SK disturbance rejection. Based on these results, Table 5 lists the estimated reaction control system performance for a mission duration of 15 years. The total amount of Xenon needed for microthruster operation represents a significant addition to the fuel budged of the mission, requiring e.g. an additional propellant tank of 110 kg capacity inside the Luxor bus (Small-GEO). Anyway, considering that the typical mass of momentum-exchange devices, such as

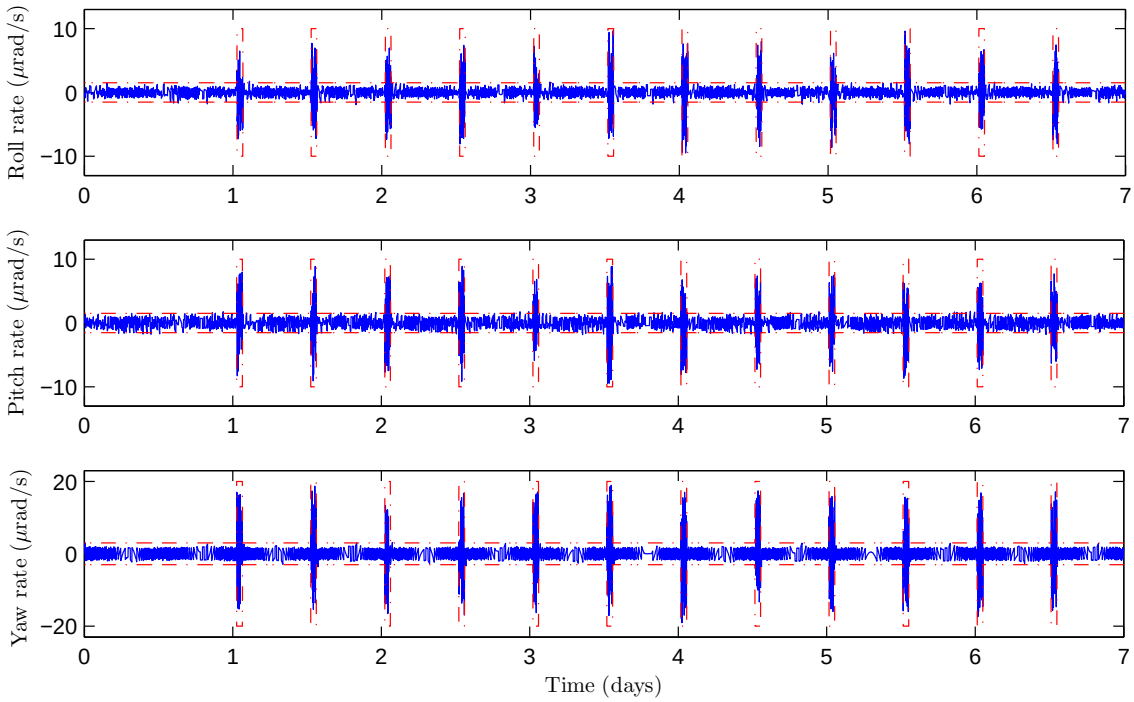

Figure 8. Pointing rate error

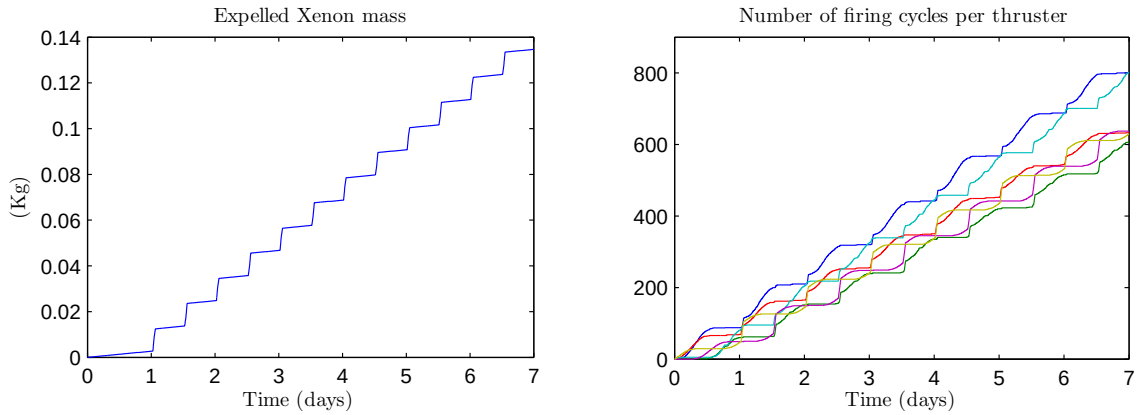

Figure 9. Microthruster reaction system performance

Table 5. Propulsion system performance for a mission duration of 15 years

Type	Xenon mass	On/off cycles	Firing time	Thermal cycles
CGT	15 (kg)	350000	300 (hr)	-
HTET	91 (kg)	300000	2000 (hr)	10000
Total	106 (kg)	650000	2300 (hr)	10000

reaction wheels or control moment gyros, together with the Xenon mass required for wheel desaturation, can easily exceed 50 kg, and that such systems are replaced by light-weight microthrusters, the resulting penalty on the spacecraft mass is predicted in the 60 kg range. It is believed that this is a reasonable trade-off as it allows one to remove moving and vibrating parts from the attitude control system, as well as to reduce its

complexity and cost. Moreover, a better alignment of the EP thrusters (using e.g. suitable thrust vectoring techniques) and/or an increased I_{sp} for HTET operation could further reduce the spacecraft mass penalty, since the amount of Xenon required for EP torques compensation scales almost linearly with these quantities. Finally, the firing time and the number of on/off and thermal cycles, given in Table 5 for a single thruster, are compatible with the considered CGT/HTET technology.

VII. Conclusions

This paper has presented an ACS for an all-electric platform equipped with Xenon microthrusters. The performance of the proposed solution in terms of pointing accuracy is suitable for both communication and Earth observation GEO missions. Simulation results have shown that fuel consumption and number of firing cycles are feasible for the reference mission, thus demonstrating that the considered technology is a viable alternative to ACS based on momentum wheels.

Although the optimization problem involved in the control law is quite challenging, the required computational power for its solution is compatible with state-of-the-art flight qualified CPUs, provided that the control horizon is kept sufficiently short. This in turn affects the control performance, and it is related to the attitude error dynamics and the pointing requirements. A detailed investigation of the trade-off between computational burden and control performance is the subject of ongoing research.

References

[1]M. De Tata, P.E. Frigot, S. Beekmans, H. Lübberstedt, D. Birreck, A. Demairé, and P. Rathsman. SGEO development status and opportunities for the EP-based small european telecommunication platform. In *32nd International Electric Propulsion Conference*, 2011.

[2]A. Krimchansky, D. Machi, S.A. Cauffman, and M.A. Davis. Next-generation geostationary operational environmental satellite (GOES-R series): a space segment overview. In *Remote Sensing*, pages 155–164. International Society for Optics and Photonics, 2004.

[3]M. Andraschko, J. Antol, S. Baize, R.and Horan, D. Neil, P. Rinsland, and R. Zaiceva. The potential for hosted payloads at NASA. In *IEEE Aerospace Conference*, pages 1–12, 2012.

[4]J.M. Shim. Korea geostationary satellite program: Communication, ocean, and meteorological satellite (COMS). In *The 2006 EUMETSAT Meteorological Satellite Conference*, 2006.

[5]J. Gonzalez and G. Saccoccia. ESA Electric Propulsion activities. In *32nd International Electric Propulsion Conference*, 2011.

[6]Boeing 702SP satellite. `http://www.boeing.com/defense-space/space/bss/factsheets/702/702SP.html`.

[7]S. Berge, A. Edfors, T. Olsson, G. Pionnier, M. Björk, C. Chasset, T. Nordebäck, M. Rieschel, B. Lübke-Ossenbeck, and P. Zentgraf. Advanced AOCS design on the first Small GEO telecom satellite. In *60th International Astronautical Congress*, 2009.

[8]T.D. Krøvel, F. Dörfler, M. Berger, and J.M Rieber. High-precision spacecraft attitude and manoeuvre control using electric propulsion. In *60th International Austronautical Congress*, 2009.

[9]Geo-Oculus final report. `http://emits.esa.int/emits-doc/ESTEC/AO6598-RD2-Geo-Oculus-FinalReport.pdf`.

[10]B Wie. Solar sail attitude control and dynamics, part 2. *Journal of Guidance Control and Dynamics*, 27(4):536–544, 2004.

[11]D. Nicolini, D. Robertson, E. Chesta, G. Saccoccia, D. Gibbon, and A. M. Baker. Xenon resistojets as a secondary propulsion on EP spacecrafts and performance results of resistojets using Xenon. In *28th International Electric Propulsion Conference*, 2003.

[12]A.N. Grubisic, S.B. Gabriel, and D.G. Fearn. Preliminary thrust characterization of the T-Series hollow cathodes for all-electric spacecraft. In *30th International Electric Propulsion Conference*, 2007.

[13]H.-D. Kim et al. COMS, the new eyes in the sky for geostationary remote sensing. *Remote Sensing–Advanced Techniques and Platforms*, pages 235–268, 2012.

[14]A. Schneider, W. Sun, and H. Schuff. The european platform luxor for small communications satellites. In *26th International Communications Satellite Systems Conference*, 2008.

[15]A. N. Grubisic. *Microthrusters based on the T5 and T6 hollow cathodes*. PhD thesis, University of Southampton, 2009.

[16]J.R. Wertz. *Spacecraft attitude determination and control*, pages 566–576. Reidel Publishing Company, 1978.

[17]M.J. Sidi. *Spacecraft dynamics and control: a practical engineering approach*, volume 7, pages 107–111. 2000.

[18]J.M. Maciejowski. *Predictive control with constraints*. Pearson education, 2002.

[19]J.L. Crassidis, F.L. Markley, and Y. Cheng. Survey of nonlinear attitude estimation methods. *Journal of Guidance Gontrol and Dynamics*, 30(1):12–28, 2007.

[20]A. Garulli, A. Giannitrapani, M. Leomanni, and F. Scortecci. Autonomous low-Earth-orbit station-keeping with electric propulsion. *Journal of Guidance Control and Dynamics*, 34(6):1683–1693, 2011.

[21]R.S. McClelland. *Spacecraft Attitude Control System Performance Using Pulse-Width Pulse-Frequency Modulated Thrusters*. PhD thesis, Virginia Polytechnic Institute and State University, 1994.